

Crystallization kinetics of the $\text{Co}_{77}\text{Si}_{11}\text{B}_{12}$ amorphous alloy

M.M. LOPACHAK¹, L.M. BOICHYSHYN^{1*}, V.K. NOSENKO², B.Ya. KOTUR¹

¹ Ivan Franko National University of Lviv, Kyryla i Mefodiya St. 6, 79005 Lviv, Ukraine

² G.V. Kurdyumov Institute for Metal Physics of the N.A.S. of Ukraine,
Akad. Vernadsky Ave. 36, 03142 Kyiv, Ukraine

* Corresponding author. E-mail: lboichyshyn@yahoo.com

Received December 2, 2020; accepted June 30, 2021; available on-line December 1, 2021

<https://doi.org/10.30970/cma14.0410>

The amorphous metal alloy (AMA) $\text{Co}_{77}\text{Si}_{11}\text{B}_{12}$ obtained by melt-spinning was investigated by X-ray diffraction (XRD) and differential scanning calorimetry (DSC) at a speed of 5, 10, and 20 K/min. The DSC curves show three stages of crystallization for all heating rates in the range of 700-900 K, which are associated with the formation of clusters and crystalline phases. The first exothermic peak, which indicates the process of nanocrystallization, occurs in the temperature range from 761 to 814 K at different heating rates. Annealing the sample for 1 h at 765 K caused changes in the XRD profile: the pre-peak at $2\theta \approx 16.5^\circ$ and the other three broad peaks at $2\theta \approx 43^\circ$, 55° and 82° became sharper, indicating the formation of different clusters in the amorphous matrix and nanocrystallization of fcc β -Co with the lattice parameter $a \approx 3.51 \text{ \AA}$ embedded in the amorphous matrix. The Kissinger method was applied for calculating the activation energies for the first, second and third DSC peaks. The activation energy E_a of nucleation and growth of nanocrystals in AMA $\text{Co}_{77}\text{Si}_{11}\text{B}_{12}$ are 347 and 374 kJ/mol, respectively. The S-like form of the dependences of the volume fraction of the crystalline phase for the first exothermic peak (α) upon temperature (T) indicates the predominance of diffusion-controlled processes at high heating rates. According to the Matusita model, the value of the growth parameter m showed that the growth of Co nanocrystals in AMA occurs by a three-dimensional mechanism, and the value of $p = 0.5$ indicates a diffusion-controlled crystallization.

Amorphous metallic alloys / Nanocrystallization / Cobalt / X-ray diffraction / Differential scanning calorimetry

Introduction

In the last two decades a variety of transition-metal-based (TM -Si-B, where $TM = \text{Fe}, \text{Co}$ or Ni) amorphous metal alloys (AMA), obtained by melt-spinning have been widely investigated. These materials exhibit excellent soft magnetic properties, for which they have wide practical application in electronics, electric transformers and sensors [1-3]. More complex alloys with a variety of properties can be obtained by adding other elements to the basic TM -Si-B ternary alloys. These properties are connected with particular structural changes occurring during the thermal treatment of the AMAs. Hence, the kinetics of crystallization of an amorphous system is a key subject to be studied. It provides opportunities to improve alloy design and processing techniques.

Magnetic properties are also significantly influenced by the size and shape of the crystalline particles. In this connection, Co-based AMAs are of particular interest. It has been shown that fine particles

of several 3d-transition elements, among which Cr and Co, often show anomalies in the phase transformation and the phase stability, resulting in metastable and unique crystal phases quite different from bulk specimens [4]. Metallic cobalt crystallizes in three different allotropic modifications: face-centered cubic (fcc) β -Co (HT phase, space group $Fm-3m$, $a = 3.545 \text{ \AA}$, stable at temperatures above 450°C), hexagonal close-packed (hcp) α -Co (LT phase, space group $P6_3/mmc$, $a = 2.507 \text{ \AA}$, $c = 4.070 \text{ \AA}$, stable below 450°C) and cubic ε -Co (space group $P4_132$, $a = 6.097 \text{ \AA}$) [5,6]. The latter metastable phase has a more complex crystal structure with 20 cobalt atoms in two crystallographic sites. Its synthesis has only been possible by means of solution-phase processes. It transforms to α -Co and β -Co during annealing of the sample at a suitable temperature [6]. All metallic cobalt phases possess interesting magnetic properties. The α -Co phase is preferable for magnetic recording applications, while β -Co is useful for applications as a soft magnetic material, due to its symmetrical low

coercivity [5]. The ideal transition temperature between the two close-packed hcp and fcc Co structures is 450°C (723 K), but in practice the energy difference between them is so small that random intergrowth of the two is common. Small temperature or pressure variations give rise to changes in the crystal structure. Several studies also have shown a strong correlation between the particle size and the crystal phase of cobalt [4,7]. Pure β -Co occurs in grains of a diameter $D \leq 200$ Å, a mixture of α -Co and β -Co for $D \sim 300$ Å, and α -Co with inclusion of a very small amount of β -Co for $D \geq 400$ Å [4].

Annealing the amorphous alloy below or near the conventional crystallization temperature usually gives rise to the formation of nano-sized crystals of the main metallic component of the AMA [2,8-11]. Understanding the kinetics of nanocrystallization of amorphous alloys provides new opportunities to control the structure, which makes it an important subject of study [9,10]. Using the appropriate heat treatment at a temperature close to the crystallization temperature, it is possible to obtain a microstructure of AMA with nanograins of crystal phase embedded in the amorphous matrix.

In this paper we present and discuss crystallization kinetics of the Co-based amorphous alloy $\text{Co}_{77}\text{Si}_{11}\text{B}_{12}$ at different heating rates.

Experimental procedure

The object of the study was an amorphous alloy $\text{Co}_{77}\text{Si}_{11}\text{B}_{12}$ obtained by the melt spinning technique in

a helium atmosphere on a massive copper wheel with a circumferential speed of about 30 m/s at the G.V. Kurdyumov Institute for Metal Physics of the N.A.S. of Ukraine. The obtained alloy was in the form of strips with thickness and width of 20-25 μm and 3 mm, respectively.

X-ray diffraction (XRD) patterns of the samples were collected on an X-ray diffractometer X'Pert Philips PW 3040/60 using $\text{Cu K}\alpha$ radiation and an X'Cellerator counter. The XRD spectra were studied for samples in the as-quenched state and annealed at elevated temperature for 1 h. The size of the nanocrystals was calculated by the Rietveld method (standard program FullProf), which was also used to describe the observed structural changes of the studied material [12].

The differential scanning calorimetry (DSC, Perkin-Elmer DSC-7) technique was used to study the crystallization of the AMA. Samples with a mass of about 15 mg were encapsulated into aluminum capsules and heated up to 900 K at different constant heating rates (5, 10, and 20 K/min). As reference plate the same empty aluminum capsule was used.

Results and discussion

Fig. 1 (lower profile, green) presents the X-ray diffraction profile of AMA $\text{Co}_{77}\text{Si}_{11}\text{B}_{12}$ for the as-quenched sample. A single, relatively broad, low maximum proves that the sample is in amorphous state.

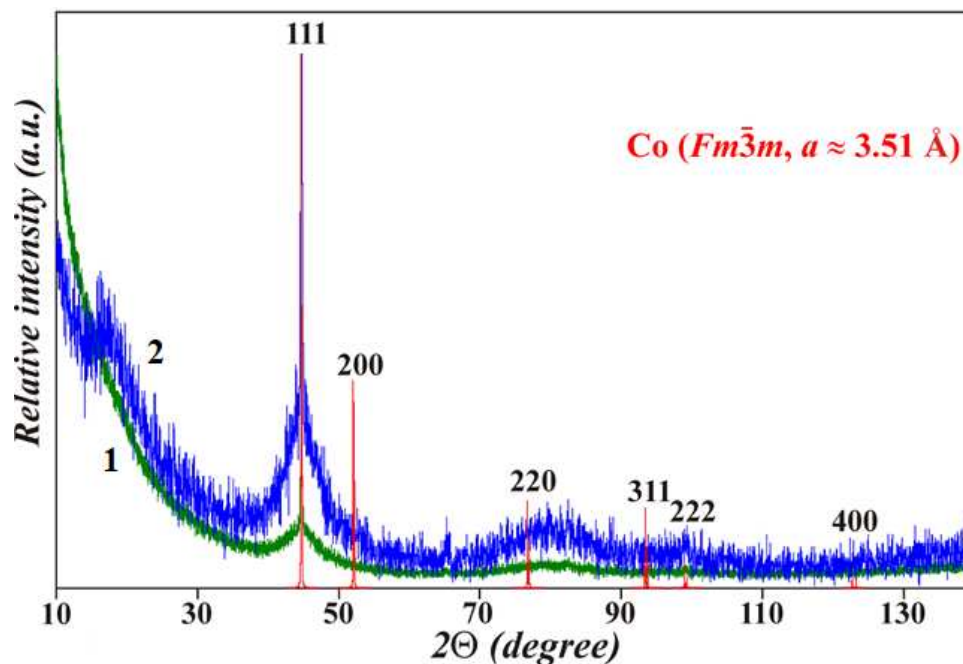


Fig. 1 XRD profiles of AMA $\text{Co}_{77}\text{Si}_{11}\text{B}_{12}$ for the as-quenched sample (lower profile, green) and for the same sample annealed at 765 K (upper profile, blue). Theoretical peaks and their hkl indices for fcc β -Co with the lattice parameter $a = 3.54$ Å are indicated.

Fig. 2 shows DSC curves of $\text{Co}_{77}\text{Si}_{11}\text{B}_{12}$ at three different heating rates: 1 – 5 K/min; 2 – 10 K/min; 3 – 20 K/min. The curves reveal three stages of crystallization for all heating rates. Increasing the heating rate shifts the peak positions to higher temperatures, *i.e.* the peak temperatures increase with increasing heating rate. This suggests that the crystallization process of the amorphous $\text{Co}_{77}\text{Si}_{11}\text{B}_{12}$ alloy should be considered as a thermally activated process, which depends on the diffusion rate of the atoms. Thus, in the range 700-900 K there are three structural transformations associated with the formation of clusters and crystalline phases. Each peak on the DSC curve is characterized by three temperatures: T_1 – temperature of nucleation; T_2 – temperature of growth; T_3 – a temperature of constant rate of formation of crystals (see Fig. 2). The first exothermic peak, which indicates nanocrystallization, occurs in the temperature range from 761 K to 814 K at different heating rates.

From Fig. 1 (upper profile, blue) it is seen that annealing of the as-quenched sample for 1 h at 765 K, the temperature of the first crystallization stage (curve 2 in Fig. 2), changed the XRD profile of the sample: a pre-peak at $2\theta \approx 16.5^\circ$ has appeared, three other peaks at $2\theta \approx 43^\circ$, 55° and 82° have become sharper, and several weak peaks have appeared, implying that a composite structure of amorphous matrix and crystalline phase has formed. The peaks associate with fcc β -Co and the lattice parameter $a \approx 3.51 \text{ \AA}$. This value is lower than for the ideal structure $a = 3.5446 \text{ \AA}$. The process of crystal formation in the investigated alloy corresponds to the first exothermic peak on the DSC curves. Thus, annealing for 1 h at $T_1 = 765 \text{ K}$ leads to the nucleation of a nanocrystalline phase of β -Co

embedded in an amorphous matrix. The pre-peak in the low-angle region may be evidence of the formation of clusters in the amorphous matrix, whose dimensions exceed the radius of the first coordination sphere of the Co atoms. The presence of a pre-peak on the diffraction patterns of annealed AMC can be associated with clusters consisting of 10-12 cobalt atoms [13], Co-Co or Co-B pairs [14]. It is also possible that Si atoms create diffusion layers or that Co-B-Co and Co-Si-Co clusters appear in the amorphous matrix [15].

Our data differ from those obtained by Stoklosa during the primary crystallization of two other ternary Co-based amorphous alloys, $\text{Co}_{80}\text{Si}_9\text{B}_{11}$ and $\text{Co}_{77}\text{Si}_{11.5}\text{B}_{11.5}$ [9,10]. Two stages of crystallization were reported, and the hexagonal α -Co phase appeared in an amorphous matrix upon annealing the samples at temperatures 748 K and 798 K, respectively. The XRD profiles for $\text{Co}_{80}\text{Si}_9\text{B}_{11}$ and $\text{Co}_{77}\text{Si}_{11.5}\text{B}_{11.5}$ differ from those of $\text{Co}_{77}\text{Si}_{11}\text{B}_{12}$ for the quenched and for the heated samples. The observed differences may be the result of different melt-spinning parameters of the amorphous samples.

The Kissinger method [16] was used to calculate the activation energies of the kinetic processes for the first, second, and third peaks of the DSC curves of the alloy (see Fig. 2). The activation energy of nanocrystallization (E_a) was obtained from the temperature dependence of the reaction rate constant: $\ln(\beta/T_x^2) = -(E_a/T_x R) + A$, where β – heating rate, K/min; E_a – activation energy, J/mol; R – universal gas constant, J/mol·K, and A – a constant; T_1 – temperature of nucleation of the nanocrystalline phase, K; T_2 – temperature of growth of the nanocrystalline phase, K; T_3 – temperature of constant rate of formation of nanocrystals, K (see Fig. 2).

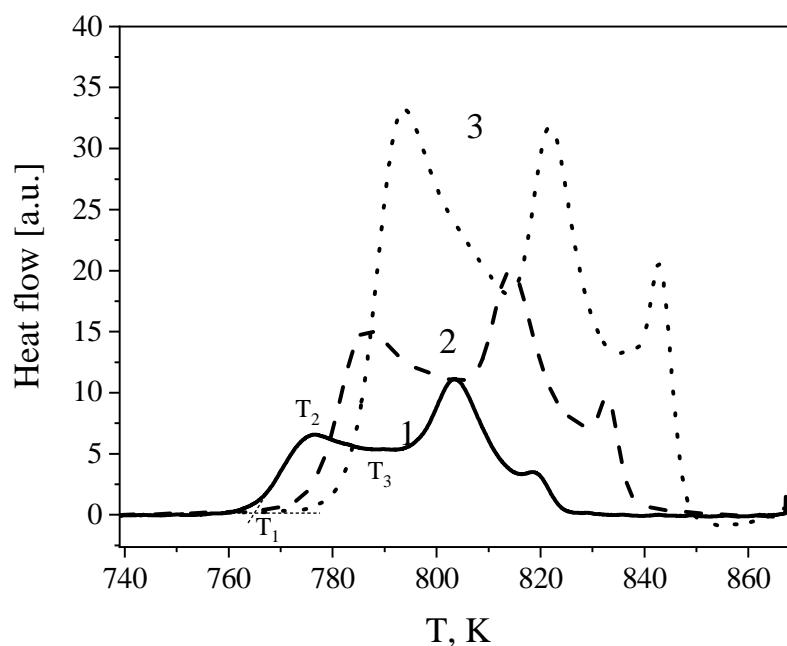


Fig. 2 DSC curves of $\text{Co}_{77}\text{Si}_{11}\text{B}_{12}$ at three different heating rates: 1 – 5 K/min; 2 – 10 K/min; 3 – 20 K/min.

The dependences are described by the equation of the line and indicate first order for the reaction of formation of Co nanocrystals in an amorphous matrix. The results of the calculations are shown in Table 1. The activation energy E_a for the first step of nanocrystallization in AMA Co₇₇Si₁₁B₁₂ is equal to 347 kJ/mol. High values of activation energy indicate complex diffusion processes in the amorphous matrix. Slightly lower values of the activation energies for the primary crystallization process were calculated by measuring the electrical resistance of AMA Co₇₇Si_{11.5}B_{11.5} at heating rates of 2, 5 and 10 K/min [10] and measuring the magnetization of an amorphous alloy Co₈₀Si₉B₁₁ at heating rates of 0.5, 2.2 and 4.4 K/min [9]; the values were 2.2 eV (211.9 kJ/mol) and 3.0 eV (289 kJ/mol), respectively.

The kinetic parameter derived from the DSC curves is the volume fraction transformed from amorphous to nanocrystalline state $\alpha = S_{1/2}/S_{\Sigma}$, where

$S_{1/2}$ is the half-area from T_1 to T_3 , and S_{Σ} is the peak area from T_1 to T_3 [17]. Fig. 3 presents plots of the volume fraction of crystalline phase (α) vs. temperature (T) for the first exothermic peak at different heating rates. The S-like shape of the dependences indicates a predominance of diffusion-controlled processes at higher heating rates.

The Matusita model differs from the Kissinger method and provides useful information about the Avrami index (n) and the dimension of growth during AMA crystallization [17]. In addition to the activation energy, this method can evaluate the mechanism of growth of crystalline phases. Kinetic parameters such as n – the Avrami index, and m , p , b from the Matusita model, were calculated according to the equation: $n = b + pm$ [18], where b is a parameter that corresponds to the nucleation rate. p is a parameter that characterizes the type of transformation, and m is the growth parameter, and are presented in Table 2.

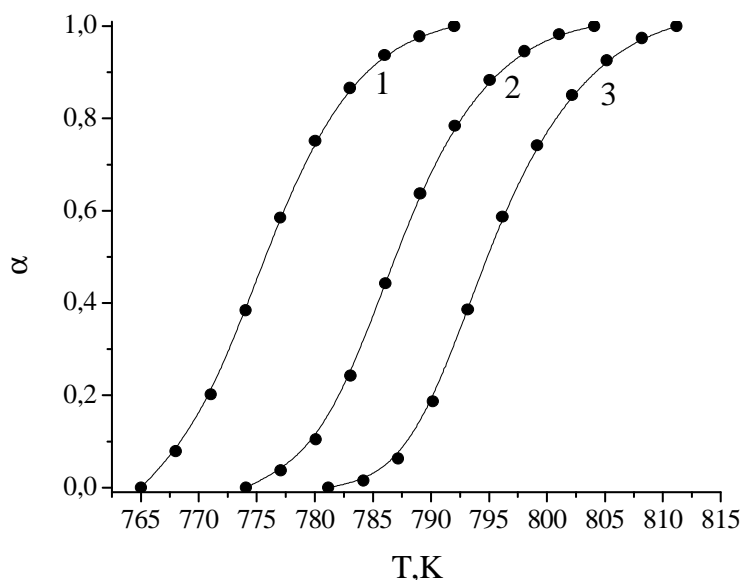


Fig. 3 Degree of crystallization (α) of AMA Co₇₇Si₁₁B₁₂ as a function of temperature at three different heating rates: 1 - 5 K/min; 2 - 10 K/min; 3 - 20 K/min.

Table 1 Temperatures of nucleation (T_1), of growth (T_2), of constant rate of formation of nanocrystals (T_3) and activation energy (E_a) of the nanocrystallization of AMA Co₇₇Si₁₁B₁₂ at different heating rates (β).

	β , K/min	T_1 , K	E_{a1} , kJ/mol	T_2 , K	E_{a2} , kJ/mol	T_3 , K	E_{a3} , kJ/mol
1 peak	5	761	347	776	374	788	266
	10	771		787		804	
	20	780		794		814	
2 peak	5	792	323	804	429	816	391
	10	804		814		829	
	20	814		821		834	
3 peak	5	816	327	819	314	827	338
	10	829		833		839	
	20	839		843		850	

Table 2 Kinetic parameters according to the Matusita model for growth of nanocrystals in the amorphous alloy Co₇₇Si₁₁B₁₂ upon the influence of temperature on the first DSC maximum.

<i>T</i> , K	<i>n</i>	<i>β</i> , K/min	<i>m</i>	<i>p</i>	<i>b</i>
779	0.6	5	1.9	1	-1.30<1
		10	2.9	0.5	-0.85<1
		20	2.7	0.5	-0.75<1

According to the average value of the growth parameter *m*, it was determined that the AMA crystallization process in the Co–Si–B system depends on the heating rate. The growth of Co nanocrystals in AMA Co₇₇Si₁₁B₁₂ at heating rates of 5, 10 and 20 K/min occurs following a 3-dimensional mechanism and the value of *p* = 0.5 indicates diffusion-controlled crystallization.

The short-range order underlying the structure of amorphous alloys is a metastable system. When heated to the crystallization temperature, the alloys tend to transform into more stable forms. As a result of thermal exposure, structural relaxation, crystallization and recrystallization occur, which can lead to the loss of favorable functional properties or, on the other hand, their improvement if a hybrid amorphous-nanocrystalline structure is formed [2,3]. As follows from the studies of AMAs based on iron [3,11,19,20] and cobalt [3,9,10] a crystalline phase is formed at the initial stage of the crystallization. This leads to radical changes of the magnetic properties and electrical resistance of the material.

Conclusions

The amorphous alloy Co₇₇Si₁₁B₁₂ was investigated by X-ray diffraction and differential scanning calorimetry at speeds of 5, 10 and 20 K/min. The curves show three stages of crystallization for all heating rates in the range 700-900 K, which are associated with the formation of clusters and crystalline phases. The first exothermic peak, which corresponds to the process of nanocrystallization, occurs in the temperature range from 761 to 814 K for different heating rates. Annealing the sample for 1 h at 765 K caused changes in the XRD profile: the pre-peak at $2\theta \approx 16.5^\circ$ and the other three broad peaks at $2\theta \approx 43^\circ$, 55° and 82° became sharper, indicating cluster formation in the amorphous matrix and nanocrystallization of fcc β -Co with the lattice parameter $a \approx 3.51 \text{ \AA}$.

The Kissinger method was applied for calculating the activation energies for the first, second and third peaks. The activation energy E_a of nucleation and growth of nanocrystals in AMA Co₇₇Si₁₁B₁₂ are 347 and 374 kJ/mol, respectively. High values of activation energy indicate complex diffusion processes in the amorphous matrix. The S-like shape of the dependence of the volume fraction of the crystalline phase for the first exothermic peak (α) upon

temperature (*T*) indicates the predominance of diffusion-controlled processes at high heating rates.

According to the Matusita model, the value of the growth parameter *m* showed that the growth of Co nanocrystals in the AMA occurred via a three-dimensional mechanism, and the value of *p* = 0.5 indicates a diffusion-controlled crystallization.

Acknowledgments

The authors are thankful to Dr. Volodymyr Levytskyi for valuable discussions and support.

References

- [1] M. Vasquez, E. Ascasibar, A. Hernando, O.V. Nielsen, *J. Magn. Magn. Mater.* 66 (1987) 37-44.
- [2] X. Zhou, H. Zhou, Z. Zhao, R. Liu, Y. Zhou, *J. Alloys Compd.* 539 (2012) 210-214.
- [3] A.V. Nosenko, V.V. Kyrlychuka, M.P. Semen'ko, M. Nowicki, A. Marusenkova, T.M. Mika, O.M. Semyrga, G.M. Zelinska, V.K. Nosenko, *J. Magn. Magn. Mater.* 515 (2020) 167328.
- [4] O. Kitakami, H. Sato, Y. Shimada, F. Sato, M. Tanaka, *Phys. Rev. B* 56 (1997) 13849-13854.
- [5] V.A.P. O'Shea, I.P.R. Moreira, A. Roldán, F. Illas, *J. Chem. Phys.* 133 (2010) 024701.
- [6] D.P. Diniega, M.G. Bawendi, *Angew. Chem., Int. Ed.* 38 (1999) 1788-1791.
- [7] H. Sato, O. Kitakami, T. Sakurai, Y. Shimada, Y. Otani, K. Fukamichi, *J. Appl. Phys.* 81 (1997) 1858-1862.
- [8] T. Mika, M. Karolus, G. Haneczok, L. Bednarska, E. Lagiewka, B. Kotur, *J. Non-Cryst. Solids* 354 (2008) 3099-3106.
- [9] S. Lesz, R. Nowosielski, B. Kostrubiec, Z. Stoklosa, *J. Achiev. Mater. Manuf. Eng.* 16 (2006) 35-40.
- [10] R. Nowosielski, A. Zajdel, S. Lesz, B. Kostrubiec, Z. Stoklosa, *J. Achiev. Mater. Manuf. Eng.* 28 (2007) 141-148.
- [11] A. Chrobak, V. Nosenko, G. Haneczok, L. Boichyshyn, M. Karolus, B. Kotur, *J. Non-Cryst. Solids* 357 (2011) 4-9.

- [12] J. Rodrigues-Carvajal, *Program FullProf*, Lab. Leon Brillouin, 1998.
- [13] Y.I. Yarmoshchuk, O.I. Nakonechna, M.P. Semenko, M.I. Zakharenko, *J. Magn. Magn. Mater.* 367 (2014) 15–18.
- [14] G. Shan, J.L. Zhang, J. Li, S. Zhang, Z. Jiang, Y. Huang, C.-H. Shek, *J. Magn. Magn. Mater.* 352 (2014) 49-55.
- [15] J. González Estévez, *Mater. Lett.* 12(3) (1991) 168-170.
- [16] H.E. Kissinger, *Anal. Chem.* 29 (1957) 1702-1706.
- [17] S. Ahmadi, H.R. Shahverdi, S.S. Saremi, *J. Mater. Sci. Technol.* 27 (2011) 497-502.
- [18] S. Ahmadi, H.R. Shahverdi, S.S. Saremi, *Iran. J. Mater. Sci. Eng.* 7 (2010) 25-29.
- [19] V. Kh. Kasiyanenko, V. L. Karbivskyy, S. S. Smolyak, O. I. Slukhovskyy, L. I. Karbovska, V. K. Nosenko, *Metallofiz. Noveishie Tekhnol.* 37(1) (2015) 37-47.
- [20] L. Boichyshyn M.-O. Danyliak, B. Kotur, T. Mika, *J. Phys. Chem. Solids.* 18 (2017) 122-128.